A Simplified Calculation Method for Heat Release Rate of Thermoplastic Combustible Materials

Norichika KAKAE[1,2], Kazunori HARADA[1,3], and Yoshifumi OHMIYA[4]

[1]*Department of Architecture and Environmental Design, Kyoto University, Yosida-Hommachi , Sakyo, Kyoto 606-8501, Japan*
[2]*COE technical staff, Tokyo University of Science*
[3]*COE visiting associate professor, Tokyo University of Science*
[4]*Department of Architecture, Tokyo University of Science, 2641 Yamazaki Noda-shi, Chiba 278-8510, Japan*

Abstract

A simplified calculation method for heat release rate of thermoplastic combustible materials was developed. The model takes into account for the variation of area of melting, stacked and burnout surfaces. All the procedure was expressed in terms of analytical formula for the convenience of use in design calculations. The calculated results were compared with three independent experiments published in literatures. In case of thin polyurethane mattress, spread of melting surface in horizontal direction was predicted fairly. However the prediction of downward spread was poor. Reflecting the errors in the position of melting surface, calculated HRR curves had some differences in their pattern. As to thick mattress, prediction of melting front was better, however the peak HRR value was underestimated because of the burning of side surfaces in experiments.

Key words: heat release rate, flame spread, fire safety engineering design, design fire source

1.Introduction*

In the modern fire safety engineering (FSE) design, design fire source is assumed to check the adequacy of fire safety measures. Quite often, heat release rate (HRR) is assumed by expert judgment; however, it is desirable to develop rational prediction method for HRR based on the potential combustibles that will exist in design object. As to the combustion and heat release rate of various combustible items, a considerable number of burning experiments were conducted so far including chairs, beds, sofa and assembly of those items.

Basic characteristics such as flame height and heat release rate are readily available in published literature [1] for specific size and shape of tested items. However, in FSE design, different size of combustibles shall have to be assumed rather than the items actually tested. Thus we need to

Corresponding Author- Tel.: +81-75-753-5779;
Fax: +81-75-753-5748
E-mail address: be.norika@archi.kyoto-u.ac.jp

extrapolate the measured HRR curves for the differences in characteristic size of tested and assumed combustibles.

This work attempts to establish a rational method to extrapolate HRR of tested items to the HRR of the items of real dimension and shape but with the same burning properties.

As a preliminary step of development, a simple prediction method was developed to scale predict time variation of HRR of thermoplastic combustibles with simple geometries using basic properties of materials. During combustion of thermoplastic material, burning surface spreads towards the edge of material, while the melted material is stacked on floor.

Assuming constant spread rate of melting surface, the change of surface area was expressed by a simple algebraic formula for cubic polyurethane material. Burning surface area was calculated by the sum of melting surface and stack area. By multiplying HRR per unit surface area with burning surface area, HRR of whole item is calculated. The calculated results are compared with experiments published in literature.

2. Theoretical Formulation

2.1 Schematics of calculation method

Figure 1 shows the dimension of combustibles item. Characteristic dimensions, namely width X, depth Y and height Z, were determined to represent size of combustible item. Global coordinates x, y, z are defined in parallel with the direction of width X, depth Y and height Z. If this item is ignited at an arbitrate position (x_0, y_0, Z) on top surface melting surface, stack surface and burnt-out surface spread as shown in Figure 2.

After ignition, melting surface spreads approximately in spherically shape for a relatively short period as shown in Figure 2a). As melting surface reaches at bottom, stacked surface is formed on the bottom in a circular region below ignition point as shown in Figures 2b) and 2c). As stacked mass is consumed, burnt-out surface is formed at the bottom of ignition point as shown in Figure 2d). Melting surface, stacked surface and burn-out surface spread in the way as shown in Figure 2e) and 2f) to burnout of whole item.

Total burning area of whole item was calculated by the sum of melting surface and stacked surface. HRR was calculated by multiplying total burning area of melted material, and by HRR of material per unit surface area, which can be obtained by cone calorimeter measurements.

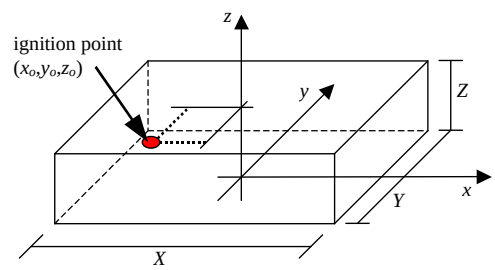

Figure 1 dimension of combustible item

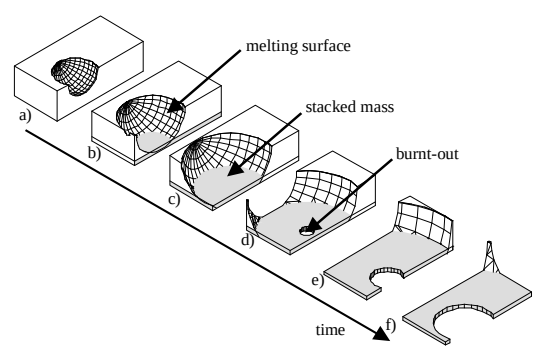

Figure 2 spread of melting, stacked and burnout surfaces

2.2 Heat release rate

As was described above, HRR is calculated by the product of burning surface and HRR per unit surface area as

$$Q = q_0 \left(A_m + A_s \right) \qquad (1)$$

where A_m is the area of melting surface, A_s= is the stacked area.

2.3 Rate of Melting Surface Spread

The rate of melting surface spread is calculated by heat balance on melting surface. The movement of melting surface towards solid part during small time interval dt is illustrated in Figure 3. Heat absorbed by melting surface is consumed to melt the surface material over the thickness of $v_m dt$ and to heat up solid material. Thus the heat balance for the small time interval would be

$$q_{net} dt = L_m \rho v_m dt + \left[\int_0^\infty \rho c_p T(x) dx \right]_t^{t+dt} \approx L_m \rho v_m dt + c_p \rho \left(T_m - T_0 \right) v_m dt \qquad (2)$$

where L_m is latent heat of melting [kJ/kg], ρ is the density of solid material [kg/m^3], c_p is specific heat [kJ/kg.K] and $T(x)$ is the temperature distribution measured along the axis perpendicular to melting surface toward solid body.

Approximating that both flame and melting surface are blackbody and convective heat transfer coefficient is given appropriately, net heat flux absorbed by melting surface is given by

$$q_{net} = \sigma \left(T_f^4 - T_m^4 \right) + h_c \left(T_f - T_m \right) \qquad (3)$$

where σ(=5.67x10^{-11}kW/m^2.K^4) is the Stefan-Boltzmann constant, T_f is flame temperature [^{o}C], T_s is the melting temperature [^{o}C] and h_c is the convective heat transfer coefficient between flame and melting surface.

Substituting equation (3) into (2), we get the rate of melting surface spread as (4) is obtained.

$$v_m = \frac{\sigma \left(T_f^4 - T_m^4 \right) + h_c \left(T_f - T_m \right)}{\rho \left\{ L_m + c_p \left(T_m - T_0 \right) \right\}} \qquad (4)$$

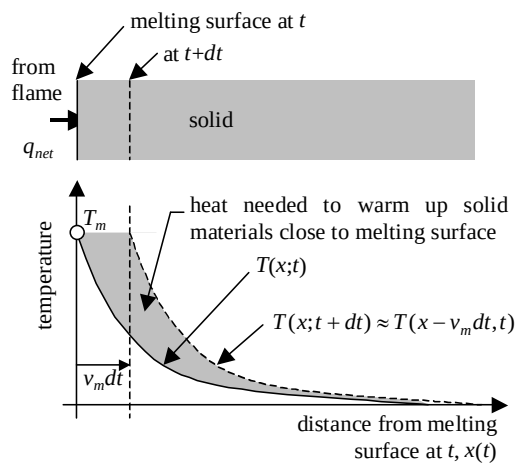

Figure 3 heat balance on melting surface

2.4 Calculation of Burning Area

2.4.1 Division of Combustibles

Theoretically it is possible to calculate burning area A_s + A_m for any geometry of item. However, for algebraic convenience, combustible item are divided into n pieces of shortcake-shaped partial cylinders with apex angle θ at ignition point as shown in Figure 4. Cylinder radii R are determined so that each cylinder volume is equal to the volume of original geometry contained within apex angle.

Then the burning area can be calculated in piece by piece as

$$A_m(t) = \sum_{j=1}^{n} A_{m,j}(t) \qquad (5)$$

where subscript j denotes the number of shortcake (j=1,2,3, …, n).

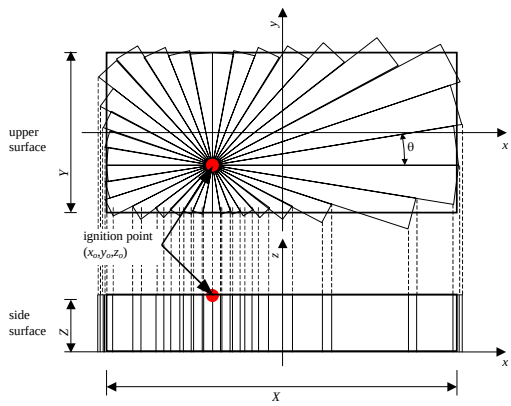

Figure 4 Division of rectangular-parallelepiped item into n pieces of shortcakes

2.4.2 Area of Melting Surface within Single Shortcake

Assuming that the rate of melting surface spread, v_m, is constant over time and invariant over directions, the area of melting surface in single shortcake can be expressed by analytical formula. At time t from ignition, melting surface locates at $r_m(=v_m t)$[m] from point of ignition. The surface area is given by the intersection of original geometry of shortcake and a sphere of radius r_m. Depending on the relative magnitude of radius R and height Z of shortcake, area of melting surface is given as functions of r_m as follows.

(1) in case of large radius $(Z \le R)$

In case of shortcakes whose radius is larger than height, melting surface first reaches at bottom, then at side surface. Thus the geometry of melting surface changes as shown in Figure 5. Until melting surface reaches bottom surface (r_m<Z), melting surface is a triangle on sphere as shown in Figure 5a). After reaching bottom surface, melting surface is a trapezoid on sphere as shown in Figure 5b). After reaching side surface as well, melting surface is again a trapezoid but the height is reduced as shown in Figure 5c). The area of melting surface is given by simple mathematics as

$$A_m(r_m) = \begin{cases} \theta r_m^2 & (r_m < R) \\ \theta(r_m - \sqrt{r_m^2 - R^2})r_m & (R \le r_m < Z) \\ \theta(Z - \sqrt{r_m^2 - R^2})r_m & (Z \le r_m) \end{cases} \qquad (6)$$

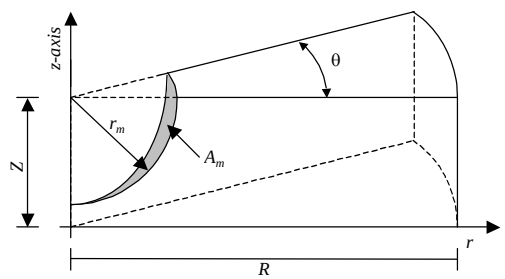

a) $r_m < Z$

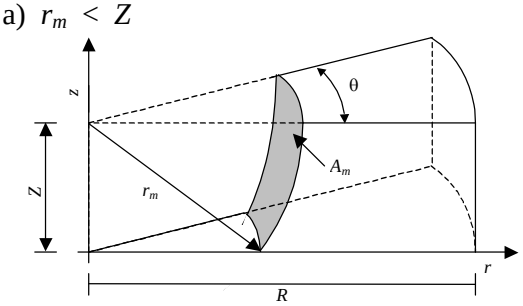

b) $Z < r_m < R$

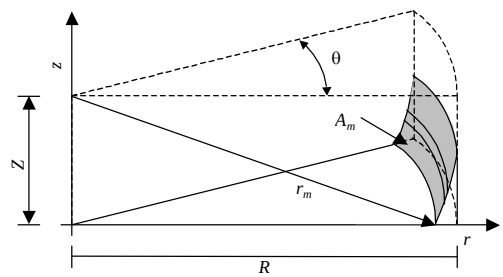

c) $R < r_m$

Figure 5 Assumed geometry of melting surface in case of $R>Z$

(2) in case of small radius $(Z \geq R)$

In case of shortcakes whose radius is smaller than height, melting surface first reaches at side surface, then at bottom. Until reaching side surface, the geometry of melting surface is the same as in Figure 5a). After that, geometry of melting surface would be as in Figure 6. Finally, after reaching bottom surface, the geometry is again the same as shown in Figure 5c). The area of melting surface is given by simple mathematics as

$$A_m(r_m) = \begin{cases} \theta r_m^2 & (r_m < R) \\ \theta(r_m - \sqrt{r_m^2 - R^2})r_m & (R \leq r_m < Z) \\ \theta(Z - \sqrt{r_m^2 - R^2})r_m & (Z \leq r_m) \end{cases} \tag{7}$$

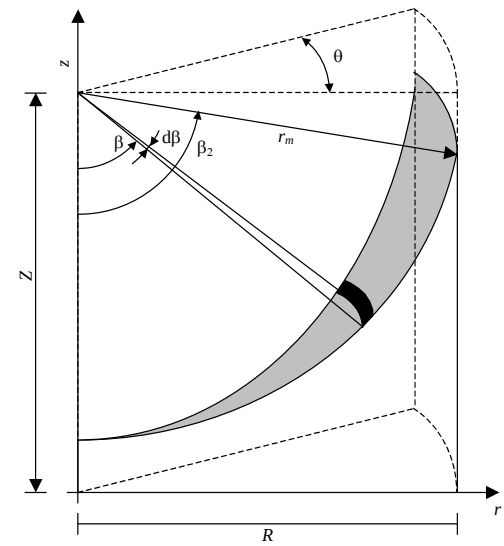

Figure 6 Assumed geometry of melting surface after reaching to arriving at a side surface and before reaching to bottom surface in case of $R<Z$

2.4.3 Area of the Stacked Surface within Single Shortcake

As shown in the hatched area in Figure 7, melted material is stacked on bottom surface. Stacked surface spreads following the spread of melting surface. At the same time, burnt-out surface spreads following stacked surface.

The sum of stacked surface area and burnt-out surface area is calculated by using the distance of melting surface from point of ignition r_m as

$$A_s + A_e = \frac{\theta}{2}\left(r_m^2 - Z^2\right) \tag{8}$$

Similarly, the area of burnt-out surface is given by replacing r_m with $r_m - v_m t_{mb}$

$$A_e = \frac{\theta}{2}\left((r_m - v_m t_{mb})^2 - Z^2\right) \tag{9}$$

where t_{mb} [s] is the duration of burning of specific position in stacked surface. Thus we get,

$$A_s = \frac{\theta}{2}\left\{r_m^2 - (r_m - v_m t_{mb})^2\right\} \qquad (10)$$

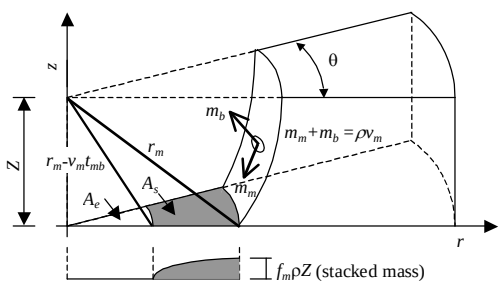

Figure 7 geometry of stacked and burnt-out surfaces

To calculate burning duration of stacked surface, mass conservation is considered. At the melting surface, mass melting rate per unit surface is equal to ρv_m.

Part of melted material is burnt on the melting surface, while the rest would drip down to bottom surface. Rate of burning can be expressed by heat of combustion per unit weight ΔH and heat release rate per unit surface q_0

$$m_b = \frac{q_0}{\Delta H} \qquad (11)$$

Thus the ratio of stacked mass generation per unit melting surface is

$$f_m = 1 - \frac{m_b}{\rho v_m} = 1 - \frac{q_0}{\Delta H \rho v_m} \qquad (12)$$

In reality, melted material drops down along the slope of melting surface. As a consequence, melted material would gather towards the point below ignition point. However, this process was neglected for simplicity but it was approximated that the melted mass would drop down to vertical direction. Under this approximation, the weight of stacked mass per unit area of bottom surface floor is $f_m \rho z$. Thus the duration of burning of stacked mass at specific point is

$$t_{mb} = f_m \rho Z \frac{\Delta H}{q_0} \qquad (13)$$

3. Comparison with Experimental Data in Literatures

In this section, comparisons were made with experimental data in literatures. Geometry and density were taken from the descriptions in literature and substituted into calculation formula. Then calculated quantities such as spread rate of melting surface and HRR were compared.

3.1 Experimental Data for Comparisons

Literature survey was carried out to collect experimental data for variety of geometry and density. So far, three experimental datasets were collected. Table 1 shows the experimental conditions. Experiments No. 1 and 2 are relatively thin mattress. In experiment No.2, specimen geometry is a triangle pole. It was ignited at apex on top surface. In experiment No.3, relatively thick mattress was ignited.

Measured HRR values are shown in Figure 8. At very initial stage of burning, HRR growth is strongly dependent on the method of ignition. Thus the induction period will be removed from experimental data so that fire growth would start at t=0 when we will compare with calculation results in the followings.

The HRR curve of thin mattress (No.1, 2) looks similar. It starts with t^2-growth, followed by linear increase. After peak

period, HRR decays linear for a while, then decreases in exponential way.

In case of thick mattress (No.3), the shape is slightly different. After the initial t^2- growth and linear growth, sharp peak period exists. Then decays to the period of constant burning period. Decay period start with linear decrease, then rapid decrease in exponential way.

Table 1 experimental condition for comparison with calculation

No.	dimension *W* x *D* x *H* [mm]	density [kg/m^3]	weight [g]	total heat release [kJ]	efficiency** *[-]	ignition point	ref.
1	500 x 500 x 140	15.7	550	14,307	0.902	center of top surface	2
2	900 x 600 x 160*	10.0	432	11,834	0.950	zenith of top surface	3
3	1000 x 500 x 300	20.8	3,120	71,746	0.797	center of top surface	4

* Triangle pole, 600(bottom edge), 900(height), 160mm(thickness)

** Efficiency is determined by measured total heat release divided by nominal total heat of combustion, THR / (density x volume x heat of combustion).

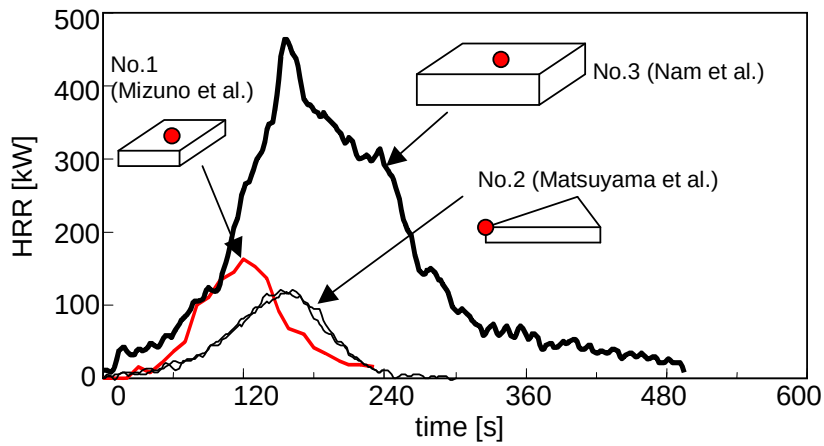

Figure 8 Experimental data for comparison with calculation

3.2 Input Parameters

The input parameters commonly used in calculations are shown in Table 2. Material properties such as heat of combustion, specific heat, melting point and heat of melting were taken from handbook values [1]. HRR per unit surface area can be taken from cone calorimeter measurements; however, average value in handbook was used.

As to empirical parameters such as convective heat transfer coefficient and flame temperature, so-called common values were used.

As shown in Table 1, combustion efficiency (measured total heat release / theoretical total heat release) differs from unity. However perfect combustion was assumed in all of the calculations.

Table 2 parameter values commonly used in the calculations

Properties of polyurethane		
Heat of combustion (ΔH)	28.9	MJ/kg
HRR of per unit area (q_0)	450	kW/m^2
Specific heat (c_p)	1.8	kJ/kg.K
Melting point (T_m)	300	^{o}C
Heat of melting (L_m)	800	kJ/kg
Empirical Parameters		
Convective heat transfer coefficient between flame and melting surface (h_c)	0.023	KW/m^2.K
Flame temperature (T_f)	800	^{o}C

3.3 Calculation results

Consideration is focused on qualitative nature of spread of burning surface and subsequent quantity of HRR. It was examined if the characteristic variation pattern can be reproduced by the formulation in the previous section and if the calculated quantity of HRR and burning area are adequate.

3.3.1 Thin Mattress

(1) Experimental Data No.1

Mizuno *et al.* measured mass burning rate of a square shaped polyurethane mattress of 500 x 500 x 140 mm ignited in center of top surface.

The spread of melting front is shown in Figure 9. Experimental data was shifted by 15 seconds to remove induction period. Burning surface arrived at the edge of top surface at 70 seconds from ignition. On the other hands, vertical spread was slow. Spread rate was calculated by equation (4) as

$$v_m = \frac{69.0}{15.7 \times 1{,}304} = 0.00337\,[\text{m/s}] \qquad (14)$$

which is shown by solid line in Figure 9. As is shown, calculated spread rate is close to horizontal spread rate, but quite larger than vertical spread rate.

Figure 10 shows geometry of melting front in comparison with measured data. In consistent with the comparison made in Figure 9, horizontal position is in fair agreement, however vertical spread is much faster in calculation than in measurement.

The HRR value was compared in Figure 11. During initial period up to 30 seconds, agreement is good. However, as the time elapses, agreement becomes worse. Because of the overestimation of burning surface, calculated HRR values are larger than experimental measurement. Peak value in calculation takes place at 60 seconds when the entire top surface was melted. After this moment, HRR decreases gradually. After 95 seconds when entire material was melted, entire bottom surface burns. Thus the HRR keeps constant value. After 135 seconds, HRR decreases gradually as burnt-out surface spreads.

Comparing with measurement, overall shape of HRR curve are not in good agreement. However the prediction of peak HRR is fair. This is because of the error in calculation of burning surface area.

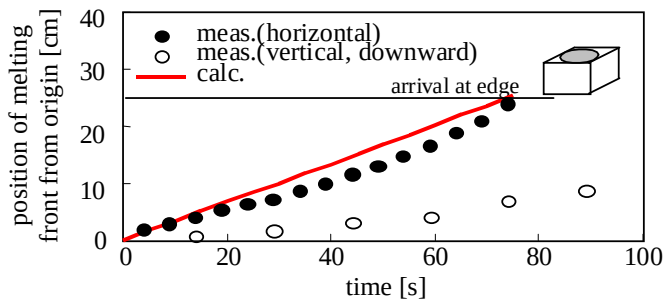

Figure 9 Comparison of spread rate of melting surface in horizontal and vertical directions in experimental data No.1 (thin square mattress, 500 x 500 x 140, Experimental data was shifted by 15 seconds.)

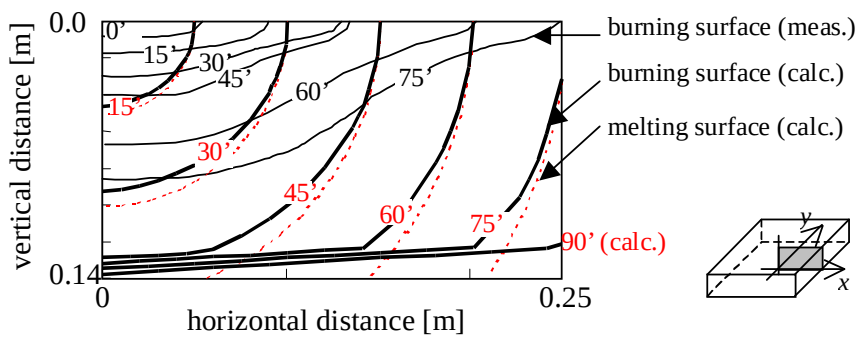

Figure 10 Comparison of burning surface at the section of symmetry axis at every 15 seconds. (thin square mattress, 500 x 500 x 140, Experimental data was shifted by 15 seconds. For the purpose of graphical presentation, the height of stacked surface was assumed to be 20 % of original material.)

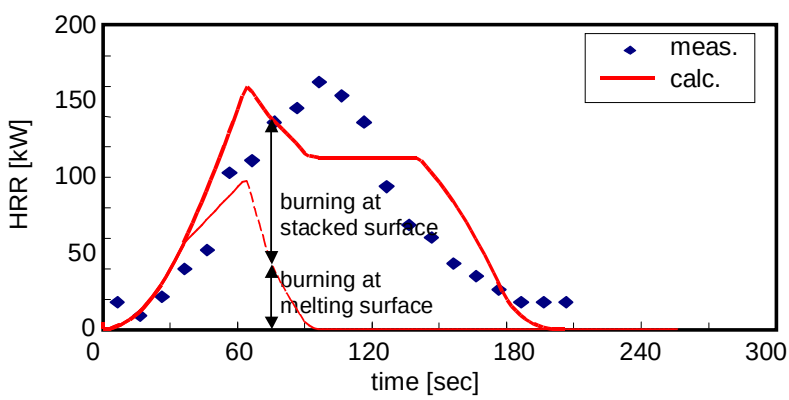

Figure 11 Comparison of calculated HRR with experimental data No.1 (thin square mattress, 500 x 500 x 140, Experimental data was shifted by 15 seconds.)

(2) Experimental Data No.2

Matsuyama *et al.* carried out an experiment for triangular shaped thin mattress. The specimen was ignited at the apex of top surface. The results are shown in Figure 12.

After ignition, HRR increased in t^2-growth until 100 seconds. After that, rate

of increase slowed down as in experimental data No.1. At 140 seconds, HRR peak value was about 120 kW. In a decay period, HRR decreased slowly until 160 seconds. After that, decreased rapidly to 200 seconds. Whole pattern of change is quite similar to experimental data No.1. The difference would be the time to peak value and duration of large HRR.

Calculated HRR is in good agreement up to 100 seconds. However, agreement is again get worse after 100 seconds. In this case, time to peak HRR agrees well, but the peak value is considerably smaller than experiment. This may be due to the burning of side surface, which is not taken into account in calculation.

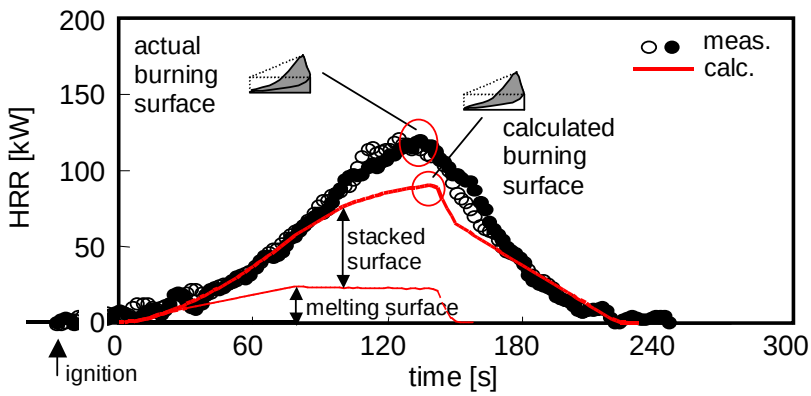

Figure 12 Comparison of calculated HRR with experimental data No.2 (thin triangle pole, 600x900x160, Experimental data was shifted by 15 seconds.)

3.3.2 Thick Mattress

Nam *et al.* measured HRR of thick mattress (500 x 1000 x 300 mm) covered by cotton cloth.

Spread of melting surface is shown in Figure 13. At 58 seconds, burning surface reached edge on top surface toward the direction of short distance. At 141 seconds, burning surface reached to farther edge top surface. Whole melting was completed at 245 seconds. After that, whole bottom area was involved with burning.

In this case, calculated spread rate of melting surface was 0.00254 m/s. Location of melting front is compared in Figure 13. It is shown that calculated velocity is approximately 20% smaller than experimental observation at top surface. As to bottom edges and corner, time to arrival is slightly small in calculation.

The HRR curves are compared in Figure 14. In experiment, HRR increased as in t^2-fire until 80 seconds. Rate of increase slows down at 80 seconds as burning surface spread at most of top surface. However, at around 120 seconds, sharp peak of HRR (approximately 460kW) exists. This is because of the burning of side surface caused by dropping of melted material along side surface. After peak value, steady burning continues to 210 seconds followed by quick decrease.

Because of its large thickness, HRR patterns in experiment No.3 differs from experiments No.1 and No.2.

In comparison with calculation, HRR in initial stage was in good agreement.

However after 80 seconds when most of the top surface is involved in burning, large difference arises. In calculation, sharp peak did not arise, but peak value remained as low as 300 kW. After peak value, HRR decreases almost linearly, followed by constant period. Then decreases exponentially. The overall pattern of HRR is in fair agreement except that calculation did not show the sharp peak value and that constant burning period is too long.

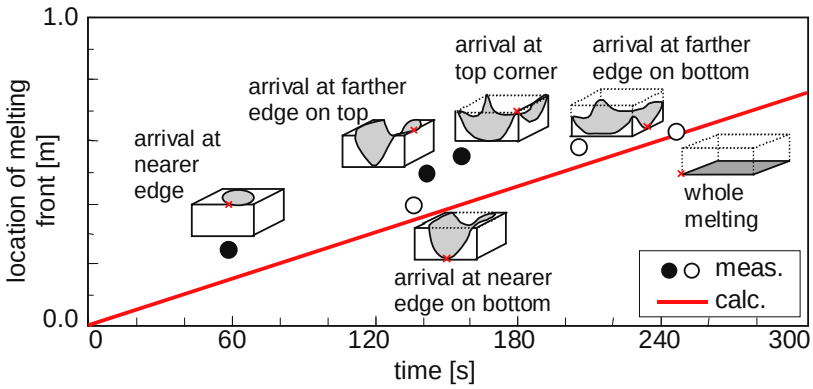

Figure 13 Comparison of calculated location of melting front with observations made during experiment No.3. (The experimental data was shifted by 25 seconds.)

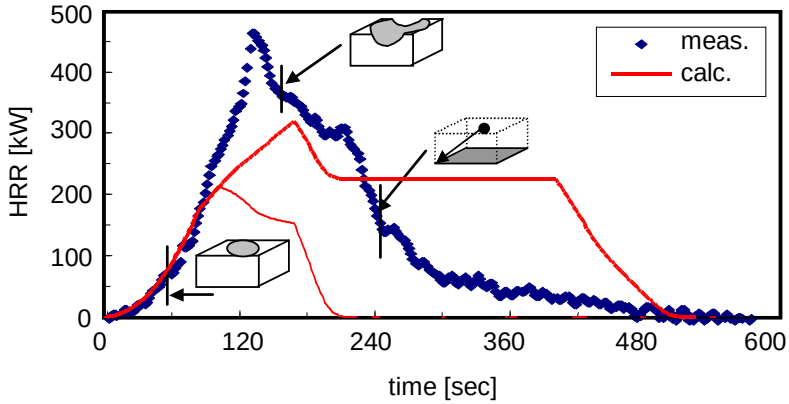

Figure 14 Comparison of calculated HRR with reference dataset No.3 (thick mattress, 1000 x 500 x 300mm. The experimental data was shifted by 25 seconds. HRR of ignition source was excluded.)

4. Conclusion

A simplified calculation method for heat release rate of thermoplastic combustible materials was developed. The model takes into account for the variation of area of melting, stacked and burnout surfaces. All the procedure was expressed in terms of analytical formula for the convenience of use in design calculations.

The calculated results were compared with three independent experiments published in literatures. In case of thin polyurethane mattress, spread of melting surface in horizontal direction was predicted fairly. However the prediction of

downward spread was poor. Reflecting the errors in the position of melting surface, calculated HRR curves had some differences in their pattern. As to thick mattress, prediction of melting front was better, however the peak HRR value was underestimated because of the burning of side surfaces in experiments.

In summary, the importance of two following aspects were suggested.

1) difference between horizontal and downward spread rate during initial period
2) spread to side surfaces during peak HRR period

which will be considered in future work in order to improve prediction accuracy.

Acknowledgements

The authors would like to thank Mr. Nam and his co-authors, Dr. Matsuyama for the information on experimental data.

Nomenclature

Alphabets

A_m	area of melting surface [m^2]
A_s	area of stacked surface [m^2]
A_e	area of burn-out surface [m^2]
c_p	specific heat [kJ/kg.K]
f_m	mass fraction of stacked material over melted material [-]
h_c	convective heat transfer coefficient [kW/m^2.K]
ΔH	heat of combustion [kJ/kg]
L_m	latent heat of melting [kJ/kg]
m_m	rate of melting per unit surface area [kg/m^2.s]
m_b	mass burning rate per unit area of melting surface [kg/m^2.s]
n	number of divisions into shortcakes
Q	heat release rate [kW]
q_{net}	net heat flux absorbed by melting surface [kW/m^2]
q_0	heat release rate per unit surface area [kW/m^2]
r_m	radius of melting surface [m]
R	radius of shortcake
t_{mb}	burning duration of stacked mass on bottom surface [s]
T_f	flame temperature [K]
T_m	melting point [K]
$T(x)$	temperature of material along an axis normal to melting surface [K]
v_m	spread rate of melting surface [m/s]
X	width of combustible [m]
Y	depth of combustible [m]
Z	height of combustible [m]

Greek letters

ρ	density of combustible [kg/m^3]
θ	apex angle [rad]
σ	Stefan-Boltzmann constant [kW/m^2.K^4]

References

[1] Society of Fire Protection Engineers, The SFPE Handbook of Fire Protection Engineering, third Edition, section 3-1, pp. 3- 37, National Fire Protection Association, 2002

[2] Tomoyuki Mizuno, Fumitaka Sasagawa, Satoru Hriuchhi, Kunio Kawagoe, “Burning Behaviour of Urethane Foam Mattress”, Fire Science and technology, Vol.1, pp.33-44, Science University of Tokyo, 1981

[3] Ken Matsuyama, Masayuki Mizuno Takao Wakamatsu, Kazunori Harada, “A Systematic Experiments of Room and Corridor Smoke Filling for Use in Calibration of Zone and CFD Fire Models for Engineering Fire Safety Design of Buildings”, Fire Science

and Technology, Vol. 21(1), pp. 43-55, Science University of Tokyo, 2001

[4] Dong-Gun Nam, Yuji Hasemi, Koji Kagiya, Masashi Yoshida, “Investigation of a Recent Large Wooden Gymnasium Fire, Part 2, Experiments for the Estimation of the Mechanism of Flashover”, Japan Association of Fire Safety Engineering, Spring Meeting, pp. 144-147, 2002